ISSN 1330-3651 (Print), ISSN 1848-6339 (Online)
https://doi.org/10.17559/TV-20240613001772
Original scientific paper

Cracking of HSLA Steel Nioval 47 Caused by Exploitation Condition and Repair Welding

Milan MILADINOV, Branislav ĐORĐEVIĆ*, Simon SEDMAK, Filip VUČETIĆ, Lazar JEREMIĆ, Aleksandar SEDMAK, Olivera POPOVIĆ

Abstract: The metallurgical characteristics of high-strength low-alloyed (HSLA) steel and the effects that could lead to crack initiation, especially in the heat affected zone, have to be taken into account during defining welding technology. Primary aim of this study is dealing with the thermal effect caused by repair welding of HSLA Nioval 47, along with the damage analysis of a water supplying pipeline made of this steel and the circumferential welded joints. Analysis has shown the involvement of different damage mechanisms on reconstructed pipeline. Thermal cycle during repair welding with a focus on cooling time ($t_{8/5}$) and with heat input (E) was thoroughly defined, along with recommended technological measures. After repair welding (using E 50 6 1 Ni B 42 electrode), microstructure analysis was performed on the surfaces at the most critical locations, i.e., the repaired circumferential welds A and B. In addition to martensite structure in the coarse-grain heat affected zone, crack initiated in the weld metal, ending at the fusion line, was detected, despite the adequately defined welding technology. One of the major remarks is related to the importance of available data needed for analysis and failure prevention during the exploitation period, guarantying reliability and safety of the pipeline.

Keywords: damage analysis; heat affected zone; heat input; HSLA steel; microstructure analysis; pipeline; repair welding

1 INTRODUCTION

Pressure equipment must be designed and manufactured in accordance with safety requirements, whereas their design work life is directly related to exploitation conditions. Developed (and implemented) standards (such as EN 13445 and EN14620), most of which are compulsory, follow these safety requirements, along with various regulations for design, production and materials selection, all of which are related to exploitation conditions. Regarding the aforementioned, standards, regulations and technical norms narrow the selection of materials to specific groups, and the ultimate goal of this is to ensure structural integrity. However, despite all of this, unpredictable aspects such as the human factor can compromise structural integrity of the system as a whole, which is further complicated by potential lack of technical documentation. This could eventually affect all design stages, but is particularly detrimental to maintenance. Current state of the material, along with its vulnerability to damage under specific exploitation conditions, including damage mechanisms, play an integral role in remaining life assessment and overhaul plans (including replacement and/or repairs of parts or entire systems) [1-5]. Components of pressure equipment are assembled and joined by welding, and significance of welded joints during structural integrity assessment is reflected by the fact that they represent "*critical*" locations in the structure itself [6, 7], especially in the case of multiple cracks presence [8].

Pressure equipment is subjected to various working conditions during its exploitation, such as internal pressure, temperature, corrosion, fatigue, etc. These conditions can lead to the most dangerous scenario - sudden brittle fracture, such as the case recorded in Boston (USA), in January 1919 [9]. Only four years after it was manufactured and started working, a huge molasses tank fractured and released an 8 m wave of its content. Investigation performed afterwards reached the conclusion that this disaster was caused by several factors, including: (i) poor manufacturing of the material, (ii) low toughness (i.e., inadequate transition temperature of used steel) and (iii) the design of the tank [8]. Novel approaches to material manufacturing, with improved chemical composition of steels, successfully decreased the number of pressure vessel disasters, but did not reduce the severity of their consequences. One such example can be found in South Africa, taking place in 1973, when an ammonia tank operating at ambient temperature exploded [9, 10]. Prior to this, the tank in question was subjected to repair welding of joints in the vicinity of the lid, in order to eliminate cracks and potential stress concentration. However, heat treatment (tempering) was not properly performed, and the steel itself did not possess the required transition temperature. In addition to the significance of properly performed heat treatment, it was easy to conclude as well that the tank parent material (C-Mn steel) [10] was not adequate for the meant exploitation conditions. Exposing pressure equipment to aggressive media can lead to damage after prolonged periods, including corrosion [4, 11, 12], hydrogen embrittlement [13, 14], cavitation [15] or erosion [3, 16, 17], while thermo-mechanical effects can also produce fatigue and/or creep [18-21]. All these damage mechanisms were more likely to occur in welded joints of every structure, not just pressure equipment. Considering everything that was said up to this point, it is necessary to consider the issues related to repairing damages to pressure equipment from multiple points of view, with three questions being of crucial importance:

(1) is it possible to replace the damaged equipment with a new part?
(2) is the reconstruction/repair welding still necessary?
(3) is this feasible and under what conditions?

The answers to the previous three questions are related to the location of the equipment in need of repair, the material it is made of and the techno-economic analysis of the whole procedure (as can be seen in [22, 23]).

Common characteristic of fine-grain structural steels is the low content of carbon (up to 0.2%) and alloying elements, along with high level of purity (low P and S content) and a microstructure with ferritic grain size ≤ 6, according to EU 103. This provides good toughness, even in case of increased mechanical properties. Regarding this, the weldability of such steels is generally good, and they can be welded using all common processes, in accordance with specific technological measures. Still, certain problems can occur despite all of the above, since weldability is defined by a large number of factors. High strength low-alloyed (HSLA) fine-grain steel Nioval 47 was developed as a promising material meant for process industry application and

oil refineries, especially for spherical storage tanks. However, welding of Nioval 47 requires somewhat high preheating temperature (T_p). The example of spherical storage tank has shown that the hydrotest itself could initiate new cracks near the welding region [24], and examples involving aggressive media exhibited poor resistance to hydrogen embrittlement, which could result in brittle fracture [25, 26]. Heat affected zone (HAZ) of a welded joint made of this HSLA steel was shown to be most critical one during welding [24, 27] and that it needs additional attention, where coarse-grain structure with lower impact energy value represents the location of possible crack initiation, followed by even ductile fracture, [28]. Nioval 47 had also shown sensitivity to strain ageing process by shifting of Charpy impact energy curves to higher temperature [29]. During the welding of fine-grain HSLA steels, temperature-time cycles are of crucial importance for achieving the required welded joint properties. These cycles are analysed using cooling time $t_{8/5}$, i.e., the time needed for the welded joint to cool from 800 °C to 500 °C, and it is during this time that conditions under which the unfavourable martensitic structure occurs could be present (Fig. 1a). In the same figure, the effect of the thermal cycles during welding process (heating and then cooling), phases with structural changes, and their effect on the mechanical and ductile properties of the HAZ of a low-alloy steel are presented. Cooling time $t_{8/5}$ is limited on one side by the occurrence of quenching (reflected by the increased hardness of the HAZ), and on the other side by an increase in transition temperature (Fig. 1b).

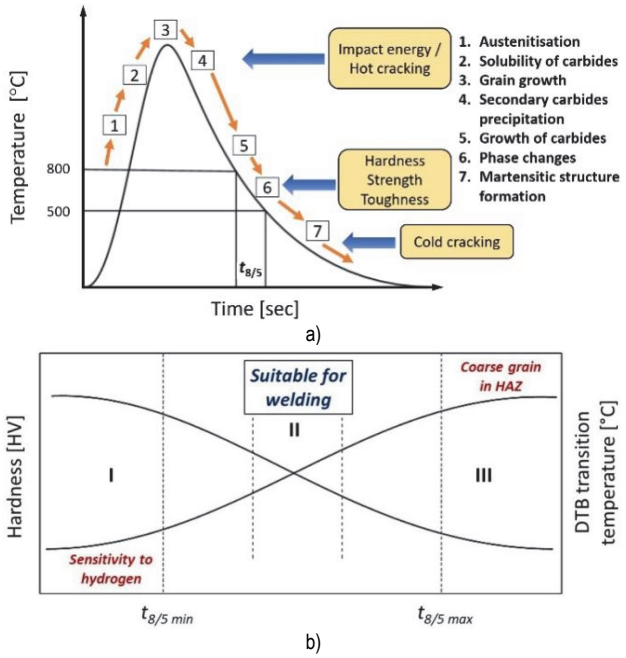

Figure 1 a) Structural changes during welding thermal cycle in HAZ of a low-alloy steel and their effect on the HAZ properties (illustration based on [30]; b) Cooling rate effect on HAZ hardness and ductile-to-brittle (DTB) transition

2 FACILITY DESCRIPTION AND DAMAGE ANALYSIS

Practical experience has confirmed that knowing about the basic mechanical properties (of material), such as tensile strength, yield stress, elongation, contraction, hardness, impact toughness, etc., is often not sufficient amount of information for properly assessing the possibility of damage and potential failure of a structure operating under different exploitation conditions. In order to successfully perform repairs which would eliminate detected damage, one must also know about previous damage to the equipment, exploitation conditions to which it was exposed, along with metallurgical properties. This chapter is devoted to describing the pipeline installation and the damage analysis.

Accumulation dam installation of the hydropower plant, where the pipeline in question is located, represents one of the largest concrete arc dams in the world. The installation is located within a mountain range and has been operating since the 1970's, mainly used for electric energy production. Due to specific topographic characteristics of the terrain, the complete installation was made beneath ground level. Water is supplied to the three turbines in the accumulation lake via three parallel pipelines, with a diameter of Ø3400 mm. Length of pipeline 1 (which is analysed here) is 277 m, from entrance to turbine axes, whereas the length of the steel part of this pipeline is ~140 m. Steel part consists of two conical transition pieces, with pipe wall thickness 24 mm. The working pressure of the pipeline is 19 bar, while the temperature of the water passing through the pipes is in rage 4-8 ºC. The pipeline consists of an upstream and downstream part, made of steel Nioval 47, according to the available documentation illustrated in Fig. 2.

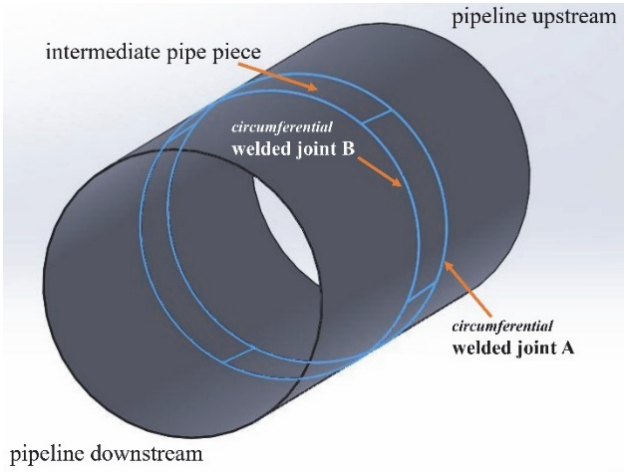

Figure 2 Pipeline number 1

An intermediate pipe piece with length of 100 mm was installed between these two parts during previously carried out reconstruction of pipeline. It was also made of Nioval 47, which was connected to the pipeline with circumferential welded joints A and B. In addition to welds A and B, intermediate pipe piece has 4 longitudinal welds, each with a length of 100 mm. All welded joints were made using electrode similar to E 50 6 1 Ni B 42 by different manufacturer. Part of the pipeline with the intermediate pipe piece and the support rim is covered by a layer of concrete which is connected and is supporter to the rocks (concrete covers approximately one third of the pipeline circumference, while the remaining part is free and accessible). Supporting rim made of basic carbon steel, welded to pipeline, has a predominantly protecting role of the intermediate pipe piece and welded joints (longitudinal and circumferential) from environmental influences. Since no defects were observed (predominantly) on circumferential welded joints between supporting rim and pipeline, no further analysis was taken on this particular pipeline part, which excluded the external (i.e. environmental) effects from further analysis.

Results of the performed chemical analysis of the parent material in the upstream and downstream parts of

the pipeline, as well as the intermediate piece, are given in Tab. 1. It can be concluded that the chemical composition of the upstream and downstream pipelines differs, as a consequence of using obviously different material batches.

Table 1 Chemical analysis results for both parts of the pipeline and the intermediate pipe piece (Nioval 47)

	Chemical element / %				
	C	Si	Mn	Cr	Ni
Upstream	0.19	0.011	1.3	0.31	/
Downstream	0.17	0.012	1.2	0.25	/
Intermediate	0.17	0.011	1.35	0.28	0.3

After seven years of exploitation after the most recent repairs and tests, NDT was performed on the internal side of the pipeline wall, at their connections to the intermediate piece. Visual testing (VT) and magnetic particle testing (MPT) were made on welded joints A and B, along with the intermediate pipe piece as a whole (100% scope). Acceptability criteria were in accordance with the recommendations of standard EN 1369:2014. A total of 13 cracks/defects with length ranging from 2-110 mm, and depth of 6-24 mm were detected. Distribution of detected cracks is illustrated in Fig. 3, whereas Tab. 2 shows their dimensions, description and position in both circumferential welds and the intermediate pipe piece. No cracks were detected in the transversal welded joints as well as in parent material of the upstream and downstream sections pipeline.

Table 2 Cracks/defects dimension, location and position

Crack number and welded joint designation	Distance from zero point / mm	Length/depth / mm	Location/remarks
Crack $1_{(A)}$	1 510	85 / 24	**Radial direction** (in welded joint A)
Crack $1_{(B)}$	1 510	10 +10 / 24	**½ in radial and ½ in longitudinal direction** (in welded joint B)
Crack $2_{(A)}$	1 870	6 / 24	**In radial direction** (in welded joint A)
Crack $3_{(A)}$	2 780	25 / 20	**In longitudinal direction** (intermediate pipe piece and weld A)
Crack $4_{(A)}$	2 810	62 / 20	**In longitudinal direction** (weld B and the intermediate pipe piece)
Crack $5_{(A)}$	2 910	35 / 20	**In longitudinal direction** (intermediate pipe piece)
Crack $6_{(A)}$	3 060	2 , 8 / 6, $_2$ (26) 3 (8) 5	**In longitudinal direction** (intermediate pipe piece)
Crack $7_{(A)}$	3 510	55 / 10	**In longitudinal direction** (intermediate pipe piece)
Crack $8_{(A)}$	4 335	45 / 8	**In longitudinal direction** (intermediate pipe piece)
Crack $9_{(A)}$	8 710	110 / 24	**In radial direction** (in welded joint A)
Crack $2_{(B)}$	8 850	14 / 24	**In radial direction** (in welded joint B)
Crack $10_{(A)}$	10 140	34 / 8	**In longitudinal direction** (intermediate pipe piece)
Crack $3_{(B)}$	10 250	10 / 24	**In radial direction** (in welded joint B)

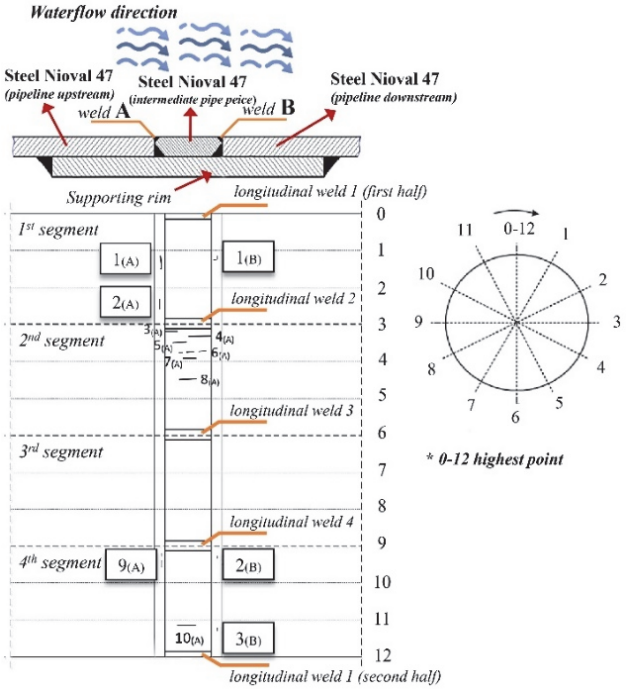

Figure 3 Distribution of cracks in the internal pipeline wall, in the intermediate pipe piece vicinity

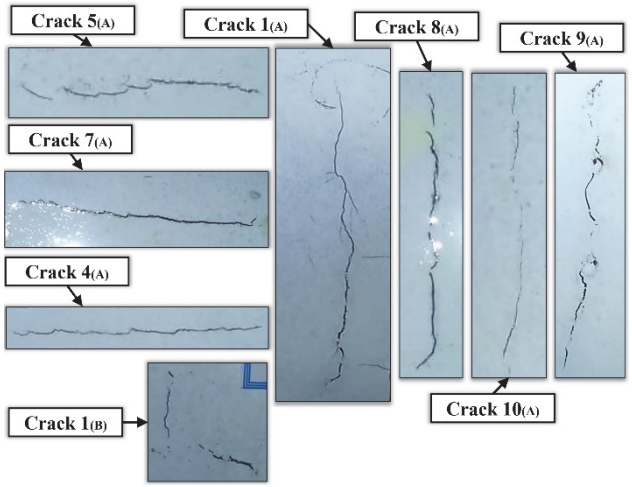

Figure 4 Appearance of some detected cracks/defects on internal pipeline wall

Detected cracks/defects in welded joints are mostly oriented along the radial direction, whereas cracks detected in the intermediate pipe piece are longitudinal. It was concluded that the longest cracks were detected in the fusion line between the upstream part of the pipeline and the intermediate piece, i.e., in welded joint A. During the previous reconstruction of the pipeline, welds A and B (as transversal welds used to connect segments) were made using basic electrode similar to E 50 6 1 Ni B 42, manufactured by Železarna Jesenice. This nickel-alloyed electrode is used for welding of non-alloyed and low-alloyed steels, as well as fine-grain steels. According to the available documentation, repair welding technology proposed preheating using a burner with propane-butane-oxygen gas

mixture, which could not achieve necessary T_p. The report, among other things, mentions that T_p was lower than required, which lead to the occurrence of local defects (cold cracks, porosity, etc.), along with residual stresses. Considering the damage found in the intermediate pipe piece parent material, it was not possible to ascertain their nature and cause, due to lack of important information. Taking into account the available documentation, installation history and the exploitation conditions of the pipeline, multiple factors could have led to crack occurrence in the parent material of intermediate pipe piece, including: (i) erosion processes; (ii) poor manufacturing technology related to rolling of the repair pieces (considering that the highest concentration of damage is located at segment 2); (iii) corrosive processes (taking into account the damage anti-corrosion later in the internal wall of the pipe at certain locations along with the properties of carbon steel used for the repair, working environment, crack geometry (Fig. 4), etc.

3 STEEL NIOVAL 47 - Properties and Weldability

This subchapter covers the properties of parent material of pipeline, steel Nioval 47, microstructure analysis and metallurgical aspects that need to be taken into account during heat input.

This steel belongs to the first generation of micro-alloyed structural steels based on C- Mn steels, with high content of these elements. Base steel used for obtaining Nioval 47 steel was steel (old JUS designation) Č0562 with R_e of 355 MPa, alloyed with vanadium (V) and niobium (Nb) in concentrations of one hundredth of a percent. The main goal of these alloying elements was to create carbon-nitrides with carbon and nitrogen, with the purpose of reinforcement of ferrite structure, by blocking dislocations. The effects of these micro-alloying elements is as follows:

- Nb builds carbon-nitrides at content levels as low as 0.005 - 0.010%, greatly increasing R_e, but decreases toughness, hence its effect needs to be countered with proper heat treatment.
- For fine-grain structural steels, V content ranges from 0.05 - 0.15% and has the same effect on rolling as Nb. Addition of V improves grain refinement, since VN nitride and VCN carbon-nitride form quicker and easier than AlN nitride. Combined effect of adding V + Nb significantly increases the R_e.

First generation micro-alloyed steels was typically formed using hot rolling, same as for regular structural steels, with one difference - temperature of final passes during hot rolling was strictly controlled, i.e., normalised hot rolling was used. This type of hot rolling with final passes was maintained in a limited temperature range, and air cooling produced the same effect as classic rolling, with the addition of normalisation annealing. Chemical composition of this steel was previously shown in Tab. 1, while the tensile properties were shown in Tab. 3.

Table 3 Tensile properties of Nioval 47 steel

$R_{p0,2}$ / MPa	R_m / MPa	A_5 / %
461	559-735	18

Nioval 47 has guaranteed toughness of 27 J at –20 °C along the transversal direction. According to standard SRPS EN 10027, this steel belongs to group 1, subgroup 1.3 (normalised steels with $R_{p0,2}$ above 360 MPa and C ≤ 0.25%. Steel P460NL1 represents the equivalent for Nioval 47 according to standard SRPS EN ISO 10025 - 3, and it is a pressure vessel steel which is more commonly used nowadays.

Microstructure of the surface layer of pipeline wall was obtained via replica method, on upstream and downstream parts of the pipeline, and can be seen in Fig. 5. Surface was etched using 8% Nital. Fig. 5 shows the fine-grain ferrite-pearlite microstructure with occasional presence of small non-metallic inclusions of the oxyde and sulfide type.

During the welding of steel Nioval 47, following risks should be considered:

- Potential occurrence of cold cracks in the weld metal and the HAZ caused by hydrogen presence.
- Potential occurrence of cracks in HAZ due to post-welding heat treatment (PWHT), i.e. quenching.
- Decrease of toughness and increase of DTB transition temperature due to forming of coarse-grains, PWHT quenching or precipitation (in HAZ).

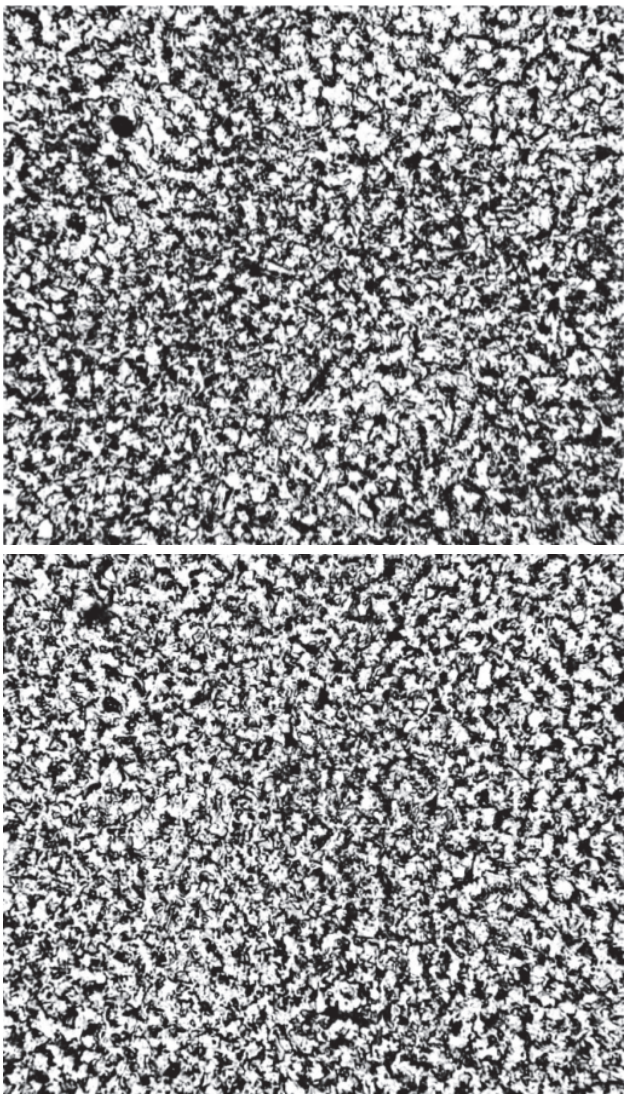

Figure 5 Microstructure of Nioval 47, sample taken from: up) upstream section of the pipeline; down) downstream section of the pipeline (magnification ×100)

During rapid cooling of Nioval 47 after welding, martensitic structure can occur, and higher presence of it in

HAZ (caused by quenching) decreases its deformability leading to cold cracks. This quenching effect can be decreased by appropriate preheating and increasing of welding energy. In addition, quenching can be significantly decreased by laying of straight, thin overlapping welds, using the technological weld for tempering of the HAZ of the previous weld, or by re-melting the finishing layer for tempering of the top of the WM. Hydrogen in the weld metal, introduced via filler material and/or the surrounding atmosphere can diffuse from the WM to the HAZ, considerably decreasing the deformability of quenched martensite, further contributing to the occurrence of cold cracks. In the WM with increased stress levels cold cracks are induced by hydrogen presence as well. In the narrow section of the HAZ, increase in grain size decreases toughness and increases DTB transition temperature. Width of this coarse-grain HAZ zone can be decreased by decreasing welding energy and T_p. To a certain extent, for multilayer welds, coarse grains can be reduced with the normalising effect of successive layers, using straight thin pass technique.

Potential precipitation of carbide and carbon-nitrides of elements V and Nb due to exposure to welding activities leads to increased R_e and R_m, but at the same time it decreases toughness and increases DTB transition temperature, hence a decrease in energy and T_p contribute to obtaining of the most favourable structures regarding toughness requirements and negative effects of precipitation.

4 THERMAL CYCLE FOR WELDING NIOVAL 47

It is well known that typical non-alloyed structural steels have good weldability if their carbon content is C < 0.25%. For the purpose of preventing the occurrence of defects and achieving of required welded joint characteristics, the most important thing is to define the conditions under which welding will be performed. Taking into account this specific HSLA steel, these conditions include:

- Defining of adequate T_p.
- Determining of temperature-time cycles for the welding process.
- Defining of PWHT.

For this type of steel, T_p can be determined using the Ito-Bessio expression [31], based on the known chemical composition of the steel, sheet thickness and diffused hydrogen content as follows:

$$T_p = 1440 \cdot P_w - 392 \text{ °C} \tag{1}$$

where P_w represents the cracking parameter determined according to the following equation:

$$P_w = C + \frac{Si}{30} + \frac{Mn}{20} + \frac{Cu}{20} + \frac{Ni}{60} + \frac{Cr}{20} + \frac{Mo}{15} + \frac{V}{10} + 5 \cdot B + \frac{s}{600} + \frac{H}{60} = 0,373\ \% \tag{2}$$

where: C, Si, Mn, Cu, Ni, Cr, Mo, V - represent the alloying elements content in %, (given in Tab. 1); s - represents the thickness (in this case, of the pipeline wall = 24 mm); $H \leq 3$ ml/100 g - represents the requirement for diffused hydrogen content in the WM.

Since $P_w > 0.24$, it is confirmed that Nioval 47 is vulnerable to cold cracking, which is already mentioned.

T_p is equal to:

$$T_p = 1440 \cdot 0,373 - 392 \text{ °C} = 145 \text{ °C} \tag{3}$$

Adopted T_p was 145-150 °C, with a recommendation for temperature increasing rate of 50 °C/h. Taking into account that there were multiple weld passes, interpass temperature (T_i) needs to be maintained at the level of minimum T_p, and for this particular material and its thickness, it is recommended to use interpass temperature of 200 °C. High T_p, which will cause heat input, would degrade the mechanical properties of the WM, such as decreasing the DTB transition temperature, whereas lower T_p than required would increase the probability of cold cracking. It is recommended that the preheating zone is 4-10× the material thickness on each side of the prepared groove.

For fine-grain structural steels, $t_{8/5}$ interval lies between 10 and 25 s according to EN 1011-2. For this steel grade, cooling should be neither too slow nor too fast, whereas slow cooling forms a coarse-grain structure in the HAZ, at the fusion line with its aforementioned negative influence. The means to determine $t_{8/5}$ depends on whether heat flow is observed as three-dimensional or two-dimensional, which is influenced by material thickness, heat input and T_p. In this specific example, heat flow is three-dimensional. It can be seen in Fig. 6 that the cooling time $t_{8/5} \approx$ 10-13 s (which is in accordance with the aforementioned interval), for preheating temperature of T_p = 145-150 °C, and heat input $E \approx$ 1.3-1.5 kJ/mm.

Thus, the heat input is calculated by Eq. (4):

$$E = \frac{U \cdot I \cdot 60}{v \cdot 1000} \text{ [kJ/mm]} \tag{4}$$

where U is current voltage, I is current amperage and v is welding speed.

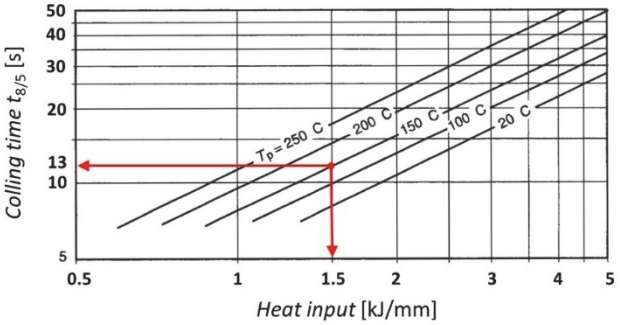

Figure 6 Cooling time $t_{8/5}$ and required E for Nioval 47

Taking all of the above into account, the following parameters were adopted for welding activities related to this steel: T_p = 145-150 °C, T_i = 200 ± 10 °C, $t_{8/5} \approx$ 10-13 s, $E \approx$ 1.3-1.5 kJ/mm.

Due to increased risk of cold cracks, it was recommended to additionaly heat the welding zone up to 200 °C over a period of 1 hour after welding was completed, in order to further eliminate diffused hydrogen from the WM. After welding, cooling must be performed gradually, for at least 5 h, with cooling rate of max 40 °C/h.

4 PARAMETERS OF REPAIR WELDING TECHNOLOGY

Field conditions imposed the need for a manual metal arc welding (MMAW) process. Taking into account the properties of parent material, an adequate welding plan and filler material selection were made, with a focus on welding parameters. Welding conditions, thermal cycle with parameters T_p, T_i, $t_{8/5}$ and E were adopted in accordance with recommendations mentioned in chapter 3.

Detected cracks/defects were previously eliminated by grinding with 3-6 mm thick grindstone. Grinding process itself was done in short intervals, without significant increase in material temperature. It was performed up to a point when the crack was no longer visible, which was verified using penetrant testing. Ground locations represent U grooves with slight radial transition, without undercuts, notches or significant changes in geometry/decrease in parent material thickness. After the groove was shaped, its dimensions were measured and it was positioned relative to the adopted reference point.

Selection of filler material was performed based on tensile properties of Nioval 47 and its vulnerability to cold cracks, thus a low-carbon basic electrode with commercial designation E 50 6 1 Ni B 42, with guaranteed hydrogen content below 5 ml/100 g in WM. This electrode is alloyed with nickel (Ni), and is meant for welding of non-alloyed and low-alloyed steels with strength up to 685 MPa, and fine-grain steels with $R_{p0,2}$ up to 460 MPa. Tensile properties and the chemical composition of this electrode are given in tables 4 and 5, respectively. Before welding, electrodes were dried in a furnace at 400 °C over 4 hours, and were then kept in a mobile "quiver" at minimum temperature 100 °C.

Table 4 Tensile properties of pure weld metal E 50 6 1 Ni B 42

$R_{p0,2}$ / MPa	R_m / MPa	A_5 / %	Av (at –40 °C) / J
> 500	560-720	> 22	> 47

Table 5 Chemical composition of E 50 6 1 Ni B 42

Element	C	Si	Mn	Ni
%	0.06	0.4	1.3	0.9

Preheating was performed by electric resistance heater, including parts of pipeline and intermediate pipe piece. Temperature was raised to 145 °C using ceramic heaters, with rate 50 °C/h. During the filling of the groove, each weld was started at the groove side, in order to use the heat input of the following pass to temper the HAZ microstructure. Final passes were laid outside of the parent material (1-3 mm for annealing of hardened zones in the parent material). It was ensured that none of the individual weld passes was shorter than 50 mm, Fig. 7. Welding parameters are shown in Tab. 6.

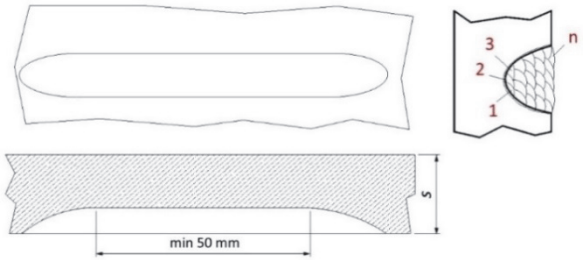

Figure 7 Illustration of U groove after machining and crack(s) elimination with filling plan

Table 6 Welding parameters

	Electrode Ø / mm	Current type	Amperage / A	Voltage / V	v / cm/min
Pass 1	2.5	DC+	70-80	23	~8.5
Fill pass 2-3	3.25		110-130	24	~13
Fill 4-n	4.0		140-160	24	~16

Temperature T_i did not exceed 210 °C. Immediately upon welding, the weld zone was reheated to 200 °C for 1 hour, to eliminate diffused hydrogen from the WM, with a cooling rate of 40 °C/h.

5 MICROSTRUCTURE ANALYSIS OF WELDS

After repair welding and reheating, NDT examination was used to verify the repair welding technology, including 100% VT, MPT and ultrasound testing (UT). These tests included repaired locations, i.e., circumferential welded joints A and B, and the ones on the intermediate pipe piece, 60 hours upon completion of welding activities. Microstructure testing was done by replica method on the surfaces of both circumferential welded joints A and B on each of four segments of intermediate pipe piece with a special attention on repaired zones (1st and 4th segment).

The VT, as well as MPT, did not reveal any defects, i.e., cracks. The UT was performed using USM 45XS device with MWB60 probe, in accordance with acceptability criteria defined by standard ISO 11666. The UT revealed cracks (minor and medium one), where one of them was spreading along few regions of weld A.

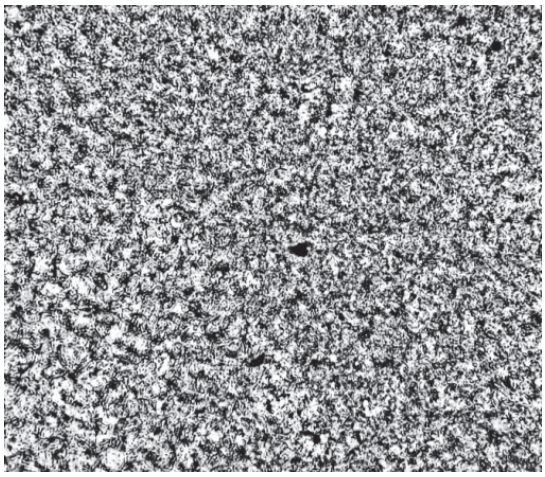

a)

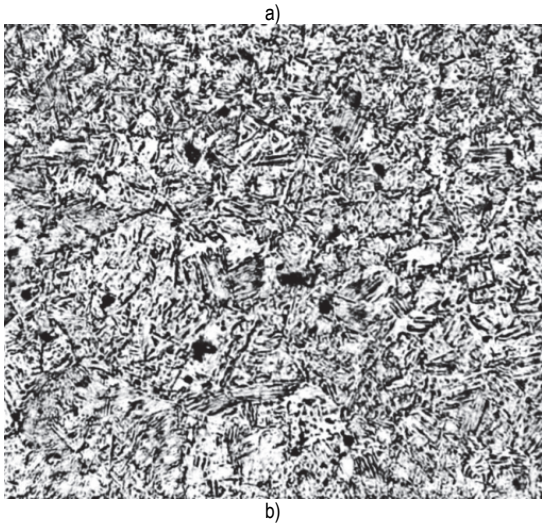

b)

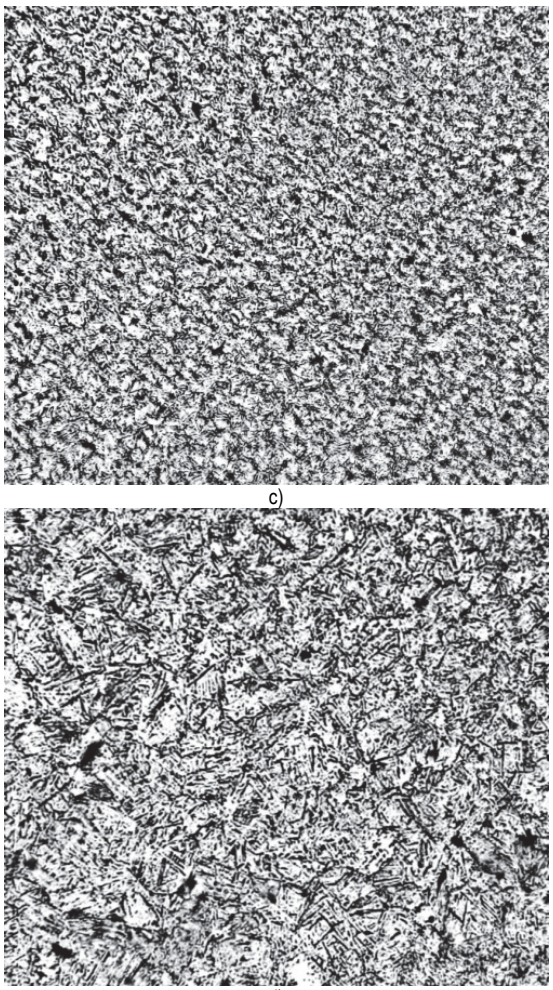

c)

d)

Figure 8 Microstructural analysis: a) weld region A: HAZ/fine-grain structure (repaired crack $1_{(A)}$); b) weld region A: HAZ/coarse-grain structure (the repaired crack $1_{(A)}$); c) weld region B: HAZ/fine-grain structure (repaired crack $1_{(B)}$; d) weld region B: HAZ/coarse-grain structure (the repaired crack $1_{(B)}$ (magnification ×100)

Microstructure analysis of the surface layer was conducted using replica method, in accordance with recommendations of SRPS ISO 3057/2011 standard. This test was performed for the purpose of determining the microstructural state of critical pipeline zones, which included welds A and B, as the most critical welds in the whole pipeline construction. Following the finishing polishing and rinsing, test surfaces were etched using 8% Nital. Analysis of microstructure was performed using the light field technique. Areas with fine-grain and coarse-grain HAZ of repaired crack $1_{(A)}$ are shown in Fig. 8a and 8b, whereas these areas in welded joint B at the repaired crack $1_{(B)}$ location are shown in Fig. 8c and 8d.

In coarse-grain HAZ region, both welds had shown presence of martensitic structure, along with individual and small and occasionally larger micropores (large black *rounds and stains* look alike marking in the Fig. 8a-d). Microstructures of the WM of both welded joints in repaired zones located in 4th segment are shown in Fig. 9. It can be seen that a bainite-ferritic microstructure is dominant in both welds, along with micropores presence. In WM of the repaired crack $9_{(A)}$, a crack with approximate length of 1.8 mm was detected (Fig. 9a-b). This crack initiated in the WM area (Fig. 9a), whereas the crack ended at the fusion line between the WM and the HAZ (Fig. 9b). Fig. 9c shows the microstructure of welded joint B of the repaired crack $2_{(B)}$.

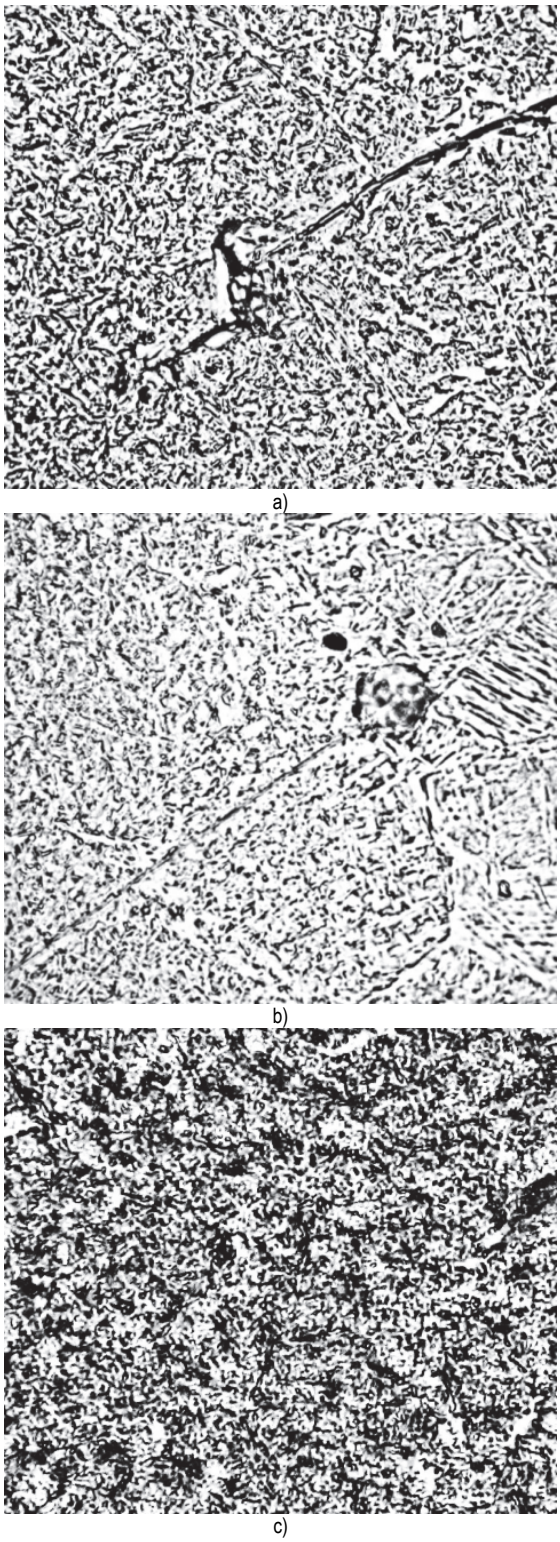

a)

b)

c)

Figure 9 Microstructure analysis: a) weld region A: weld metal - crack initiation location (the repaired crack $9_{(A)}$; magnification ×500); b) weld region A: crack ending at the fusion line between the WM and the HAZ (the repaired crack $9_{(A)}$; magnification ×500); c) weld region B: weld metal (the repaired crack $2_{(B)}$; magnification ×200)

6 CONCLUSION

One of the major remarks of this study is related to the importance of available data needed for appropriate analysis and failure prevention during the exploitation period,

which guarantee security, reliability and safety of the pipeline. Damage analysis revealed that cracks occurrence in circumferential welded joints and the parent material of the intermediate pipe piece were directly caused by insufficient T_p and poor parent material quality, respectively.

Welding of HSLA steel Nioval 47 itself demands a series of technological measures directly related to temperature and E, in order to prevent unwanted WM and HAZ microstructures (mainly coarse-grain ones). The following conclusions can be made based on the presented study:

(1) Multiple layers are required for welding Nioval 47, i.e., by applying as many thin layers as possible, without electrode sway, at optimal speed, and in accordance with recommendations for E.
(2) T_i must be maintained below 200 °C, whereas T_p should be kept within the interval of 145-150 °C, below T_i.
(3) Weld pass laying dynamics must be in accordance with prescribed work temperature, designed by the weld thermal cycle.
(4) During filling the groove, welding should begin at the side of the groove (if applicable), and finishing welds should be laid outside of the parent material in order to avoid the forming of coarse-grain HAZ.
(5) This cooling time was 10-13 s for calculated T_p of 145-150 °C and heat input of E ≈ 1.3-1.5 kJ/mm, which further determine the v.

Despite thoroughly performed analysis and defining of recommendations for the welding thermal cycle, martensite was detected in the coarse-grain HAZ in both circumferential welds in the repaired zone. Individual small and occasionally larger micropores were also observed. As for the weld metal, bainite-ferritic microstructure was the dominant one, whereas a crack with an approximate length of 1.8 m was detected in welded joint A. This crack initiated in the weld metal and ended at the fusion line. Although criteria defined by standards was fulfilled (in terms of dimensions), this crack needs to be monitored by at least one surface and volumetric NDT method, considering it was detected in a critical location in two welded joint regions (WM and HAZ). In addition, frequent monitoring period is recommended, at intervals of 6 months between two inspections. These intervals can be increased gradually if the results are shown to be satisfactory.

7 REFERENCES

[1] Jarić, M., Budimir, N., Petronić, S., Sedmak, S., & Vitas, N. (2024). Analysis of remediation of manifold line damaged by longitudinal crack in the piping elbow of oil and gas well collector. *Structural integrity and life*, *24*(1), 111-115. https://doi.org/10.69644/ivk-2024-01-0111

[2] Vojvodic Tuma, J. & Sedmak, A., (2004). Analysis of the unstable fracture behaviour of a high strength low alloy steel weldment.*Engineering Fracture Mechanics*, *71*(9-10), 1435-1451. https://doi.org/10.1016/S0013-7944(03)00166-8

[3] Jovanović, A., Đorđević, B., Jeremić, L., Milovanović, N., & Smoljanić, T. (2022). Integrity assessment of autoclaves after reconstruction. *Structural integrity and life*, *22*(3), 347-352.

[4] Lazić, V. et al. (2009). Reparation of the damaged forging hammer mallet by hard facing and weld cladding.*Tehnički vjesnik*, *16*(4), 107-113.

[5] Brautigam, A., Szalai, S., & Fischer, F. (2023). Investigation of the application of austenitic filler metals in paved tracks for the repair of the running surface defects of rails considering field tests. *Facta universitatis Series: Mechanical engineering*. https://doi.org/10.22190/FUME230828032B

[6] Bulatović, S., Aleksić, V., Milović, Lj., & Zečević, B. (2023). Experimental determination of the critical value of the J-integral that refers to the hsla steel welded joint. *Tehnički vjesnik*, *30*(1), 148-152. https://doi.org/10.17559/TV-20220419093052

[7] Jeremić, L., Sedmak, A., Petrovski, B., Đorđević, B., & Sedmak, S. (2020). Structural integrity assessment of welded pipeline designed with reduced safety. *Tehnički vjesnik*, *27*(5), 1461-1466. https://doi.org/10.17559/TV-20200413142538

[8] Arandjelovic, M., Djordjevic, B., Sedmak, S., Radu, D., Petrovic, A., Dikic, S., & Sedmak, A. (2024).Failure analysis of wel-ded joint with multiple defects by extended finite element method and engineering critical analysis. *Engineering failure analysis*, *160*, 108176. https://doi.org/10.1016/j.engfailanal.2024.108176

[9] Benac, D. J., Cherolis, N., & Wood, D. (2016). Managing cold temperature and brittle fracture hazards in pressure vessels. *Journal of failure analysis and prevention*, *16*, 55-66. https://doi.org/10.1007/s11668-015-0052-3

[10] Lonsdale, H. (1975). Ammonia Tank Failure - South Africa. in Ammonia Plant Safety (AIChE).

[11] Wasim, M. & Djukic, M. (2022). External corrosion of oil and gas pipelines: A review of failure mechanisms and predictive preventions. *Journal of natural gas science and engineering*, *100*, 104467. https://doi.org/10.1016/j.jngse.2022.104467

[12] Yang, Y., Li, W., & Liang, B. (2024). External corrosion analysis of gas pipeline based on gray prediction models. *Journal of failure analysis and prevention*. https://doi.org/10.1007/s11668-024-01909-7

[13] Djukic, M., Bakic, G., Sijacki Zeravcic, V., Sedmak A., & Rajicic, B. (2019). The synergistic action and interplay of hydrogen embrittlement mechanisms in steels and iron: Localized plasticity and decohesion. *Engineering fracture mechanics*, *216*, 106528. https://doi.org/10.1007/s11668-024-01909-7

[14] Pardal, J. M., Tavares, S. S. M., Barbosa, B. A. R. S., Mainier, F. B., Corte, J. S., & Pardal, J. P. (2013). Investigation of hydrogen embrittlement failure in a steam separator by field metallography. *Engineering failure analysis*, *35*, 46-53. https://doi.org/10.1016/j.engfailanal.2012.11.001

[15] Miladinov, M., Đorđević, B., Sedmak, S., Bratu, C., Radu, D., Sedmak, A., & Aleksić, N. (2024). Damage analysis and restoring of structural integrity of pelton runner after repair welding: case study. *Structural integrity and life*, *24*(2), 217-221.

[16] Klein, U., Zunkel, A., & Eberle, A. (2014). Breakdown of heat exchangers due to erosion corrosion and fretting caused by inap-propriate operating conditions. *Engineering failure analysis*, *43*, 271-280. https://doi.org/10.1016/j.engfailanal.2014.03.019

[17] Chen, Y., Dong, S., Zang, Z., Gao, M., Zhang, H., Ao, C., Liu, H., Ma, S., & Lium, H, (2021). Collapse failure and capacity of subsea pipelines with complex corrosion defects. *Engineering failure analysis*, *123*, 105266. https://doi.org/10.1016/j.engfailanal.2021.105266

[18] Hoseinzadeh, S. & Stephan Heyns, P. (2020). Thermo-structural fatigue and lifetime analysis of a heat as a feedwater heater in power plant. *Engineering failure analysis*, 104548. https://doi.org/10.1016/j.engfailanal.2020.104548

[19] Mateiu, H., Fleşer, T., & Murariu, A. (2010). Creep-fatigue interaction assessment of 16Mo5 steel. *Structural Integrity and Life*, *10*(29), 83-88.

[20] Négyesi, M., Kraus, M., Mareš, V., Kwon, D., & Strnadel, B. (2023). Creep damaged microstructure and mechanical properties of Cr-Mo-V steel subjected to long-term service exposures. *International journal of pressure vessels and piping*, *206*, 105085.
[21] Milovic, Lj. et al. (2008).Study of the simulated heat affected zone of creep resistant 9-12% advanced chromium steel, *Materials and Manufacturing Processes*, *23*(6), 597-602. https://doi.org/10.1080/10426910802160544
[22] Jovanović, A., Đorđević, B., Jeremić, L., Sedmak, S., & Petrović, A. (2023). Inspection of damage and risk analysis of containers in a coal drying facility in exploitation. *Structural Integrity and Life*, *23*(2), 111-115.
[23] Arsić, D., Nikolić, R., Lazić, V., Aleksandrović, S., Radović, L., Ilić, N., & Hadzima, B. (2021). An example of reparatory surface welding of the mining machine vital part. *Communication - Scientific Letters of the University of Zilina, 23*(1), B39-45. https://doi.org/10.26552/com.C.2021.1.B39-B45
[24] Kurai, J. & Aleksić, B. (2003). Proof pressure test as a cause of crack occurrence in pressurized equipment in service. *Structural integrity and life*, *3*(2), 65-71.
[25] Ažman, S., Marčetič, M., & Bernetič, J. (2013). Using aspects for welded constructions of hsla structural steels first generation with high ceq and second generation with low C_{eq}. *Welding and welding construction*, *1*, 23-30.
[26] Jovičić, R., Prokić-Cvetković, R., & Popović, O. (2005). Non-destructive testing of ferritic-austenitic welded joints. *Structural integrity and life*, *5*(3), 119-128.
[27] Tomków, J., Landowski, M., & Rogalski, G. (2022). Application possibilities of the S960 steel in underwater welded structures. *Facta universitatis Series: Mechanical engineering*, *20*(2), 199-209. https://doi.org/10.22190/FUME210722066T
[28] Filipovic, N. & Geric, K. (2006). Brittle and Ductile Fracture in Service of Pressure Vessels. *Fracture of nano and engineering materials and structures.* https://doi.org/10.1007/1-4020-4972-2_531
[29] Vojvodič Tuma, J. & Šuštaršič, B. (2006).Fracture mechanics investigations of structural steels with the yield stresses between 265 and 1000 MPa. *International Conference on Crack Paths (CP 2006)*.
[30] Radaj, D. (1992). *Heat effects of welding: Temperature Field, Residual Stress, Distortion*. Springer Berlin Heidelberg. https://doi.org/10.1007/978-3-642-48640-1
[31] Ito, Y. & Bessyo, K. (1972). Weld crackability formula of high strength steels. *Journal of iron and steel research interna-tional*, *13*, 916-930.

Contact information:

Milan MILADINOV, MSc Mech. Eng.
Metal Rehabilitation and Testing Ltd, Belgrade,
Danila Ilića 2 ,11060 Belgrade, Serbia
E-mail: miladinovmilan@gmail.com

Branislav ĐORĐEVIĆ, PhD, Scientific Associate
(Corresponding author)
Innovation Center of Faculty of Mechanical Engineering,
Kraljice Marije 16, 11120 Belgrade, Serbia
E-mail: brdjordjevic@mas.bg.ac.rs

Simon SEDMAK, PhD, Scientific Associate
Innovation Center of Faculty of Mechanical Engineering,
Kraljice Marije 16, 11120 Belgrade, Serbia
E-mail: ssedmak@mas.bg.ac.rs

Filip VUČETIĆ, PhD, Scientific Associate
Innovation Center of Faculty of Mechanical Engineering,
Kraljice Marije 16, 11120 Belgrade, Serbia
E-mail: fvucetic@mas.bg.ac.rs

Lazar JEREMIĆ, PhD, Scientific Associate
Innovation Center of Faculty of Mechanical Engineering,
Kraljice Marije 16, 11120 Belgrade, Serbia
E-mail: laki991@hotmail.com

Aleksandar SEDMAK, PhD, Professor Emeritus
University of Belgrade, Faculty of Mechanical Engineering,
Innovation Center of Faculty of Mechanical Engineering
Kraljice Marije 16, 11120 Belgrade, Serbia
E-mail: asedmak@mas.bg.ac.rs

Olivera POPOVIĆ, PhD, Full Professor
University of Belgrade, Faculty of Mechanical Engineering,
Kraljice Marije 16, 11120 Belgrade, Serbia
E-mail: opopovic@mas.bg.ac.rs